Infrared ellipsometry study of the confined electrons in a high-mobility -Al_2O_3/$SrTiO_3$ heterostructure

2016 EPL 113 47005

(http://iopscience.iop.org/0295-5075/113/4/47005)

A Letters Journal Exploring the Frontiers of Physics

February 2016

EPL, **113** (2016) 47005 www.epljournal.org
doi: 10.1209/0295-5075/113/47005

Infrared ellipsometry study of the confined electrons in a high-mobility γ-Al_2O_3/$SrTiO_3$ heterostructure

M. Yazdi-Rizi[1], P. Marsik[1], B. P. P. Mallett[1], A. Dubroka[2], D. V. Christensen[3], Y. Z. Chen[3], N. Pryds[3] and C. Bernhard[1]

[1] *University of Fribourg, Department of Physics and Fribourg Center for Nanomaterials Chemin du Musée 3, CH-1700 Fribourg, Switzerland*
[2] *Department of Condensed Matter Physics, Faculty of Science and Central European Institute of Technology, Masaryk University - Kotlářska 2, 61137 Brno, Czech Republic*
[3] *Department of Energy Conversion and Storage, Technical University of Denmark, Risø Campus 4000 Roskilde, Denmark*

received on 17 February 2016; accepted by M. Potemski on 3 March 2016
published online 14 March 2016

PACS 78.20.-e – Optical properties of bulk materials and thin films
PACS 78.67.-n – Optical properties of low-dimensional, mesoscopic, and nanoscale materials and structures
PACS 78.30.-j – Infrared and Raman spectra

Abstract – With infrared ellipsometry we studied the response of the confined electrons in γ-Al_2O_3/$SrTiO_3$ (GAO/STO) heterostructures in which they originate predominantly from oxygen vacancies. From the analysis of a so-called Berreman mode, that develops near the highest longitudinal optical phonon mode of $SrTiO_3$, we derive the sheet carrier density, N_s, the mobility, μ, and the depth profile of the carrier concentration. Notably, we find that N_s and the shape of the depth profile are similar as in $LaAlO_3$/$SrTiO_3$ (LAO/STO) heterostructures for which the itinerant carriers are believed to arise from a polar discontinuity. Despite an order of magnitude higher mobility in GAO/STO, as obtained from transport measurements, the derived mobility in the infrared range exhibits only a twofold increase. We interpret this finding in terms of the polaronic nature of the confined charge carriers in GAO/STO and LAO/STO which leads to a strong, frequency-dependent interaction with the STO phonons.

Introduction. – The observation that highly mobile electrons can be created at the interface between the nominal band-insulators $SrTiO_3$ (STO) and $LaAlO_3$ (LAO) with $\Delta_{\rm gap}^{\rm STO} = 3.2\,{\rm eV}$ and $\Delta_{\rm gap}^{\rm LAO} = 5.6\,{\rm eV}$, respectively, has initiated intense research activities on LAO/STO heterostructures [1]. Meanwhile, it has been demonstrated that functional field effect devices can be made from these oxide heterostructures [2] which even allow one to tune a superconductor to insulator quantum phase transition at very low temperatures [3]. A major unresolved question concerns the origin of these confined charge carriers and the conditions for obtaining a high mobility. The explanations range from i) an electronic reconstruction due to the polar discontinuity at the LAO/STO interface which gives rise to a transfer of 1/2 e charge per STO unit cell (corresponding to a sheet carrier density of $N_s = 3.3 \times 10^{14}\,{\rm cm}^{-2}$), ii) an intermixing of La and Sr cations across the interface [4], to iii) the creation of oxygen vacancies which may be stabilized near the interface by space charge effects [5]. While the polar discontinuity scenario (i) has obtained a great deal of attention, more recently the focus has shifted toward the oxygen vacancies (iii). In particular, it has been demonstrated that an electron gas can be created in the absence of a polar discontinuity, for example at the LAO/STO (110) interface [6], with amorphous LAO cap layers [7,8], and even with a γ-Al_2O_3 (GAO) top layer which has a spinel structure. The results reported in ref. [9] suggest that both the oxygen vacancies and the polar discontinuity can be the source of mobile electrons that are confined near the surface of STO. Notably, the highest mobility reported to date has been achieved in GAO/STO heterostructures for which oxygen vacancies seem to be at the heart of the interfacial electrons [10,11]. This raises the question

about the differences in the dynamical properties of the interfacial electrons and also of the concentration depth profiles in these different kinds of heterostructures. In GAO/STO the latter has so far only been determined at room temperature using X-ray photoelectron spectroscopy (XPS) [10,12]. The depth distribution of the confined electrons at low temperature, where the dielectric constant of STO is much larger and the electron mobility strongly enhanced, is yet unknown. Some of us have previously shown for the case of LAO/STO that this information can be obtained with infrared ellipsometry [13]. Here we present a similar ellipsometry study of GAO/STO.

Sample growth and characterization. – Two GAO/STO heterostructures with GAO layer thicknesses of 2.5 and 2.75 unit cells (in the following they are denoted as GAO-2.5 and GAO-2.75) have been grown by pulsed laser deposition (PLD) on singly TiO_2-terminated (001) STO crystals with a repetition rate of 1 Hz and a laser fluence of 2.5 J cm^{-2}, and monitored by *in situ* high-pressure RHEED [10]. During the deposition at 600 °C, the static oxygen pressure was kept constant at 10^{-4} mbar. After the deposition, the sample was cooled down to room temperature at the deposition pressure without any further post oxygen annealing. The samples have been studied with standard dc Hall transport measurements. The obtained values for the sheet carrier density, N_s, and the mobility, μ, are shown in fig. 1. The infrared ellipsometry measurements have been performed with a home-built setup that is equipped with a He flow cryostat and attached to a Bruker 113V Fast Fourier spectrometer as described in ref. [14]. The data have been taken at 10 K in rotating analyser mode, with and without a static compensator based on a ZnSe prism. Almost identical data (not shown) have been obtained by using a rotating compensator with a ZnSe prism. The angle of incidence of the light was set to 75°. Special care was taken to avoid photo-doping effects by shielding the sample against visible and UV light [15]. The measurements have been performed under identical conditions first on the GAO/STO heterostructures and, right afterwards, on a bare STO substrate that serves as a reference.

Experimental results. – Infrared ellipsometric spectra contain valuable information about the properties of the electrons that are confined at the interface of the GAO/STO heterostructure. The most instructive feature is due to a so-called Berreman mode that occurs in the vicinity of the plasma frequency of the highest longitudinal optical (LO) phonon mode [16,17] which in STO is located at ω_{LO}(STO) $\approx 788\,\mathrm{cm}^{-1}$ [18]. It is an electronic plasma mode that originates from a charging of the interfaces due to the dynamical accumulation of the itinerant charge carriers. It occurs under an oblique angle of incidence of the light if the polarization of the electric field, E, is parallel to the plane of incidence (p-polarization) and thus has a finite normal component with respect to the interfaces. The corresponding reflection coefficient, r_p, exhibits

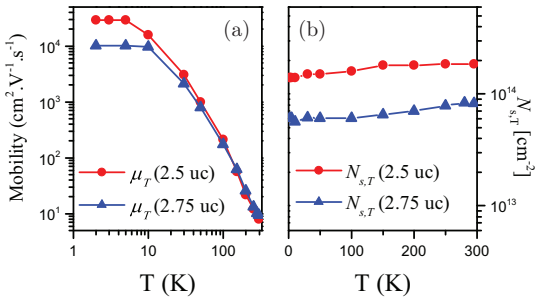

Fig. 1: (Colour online) Temperature dependence of (a) the mobility, μ, and (b) the sheet carrier density, $N_{s,T}$, as obtained from dc transport measurements on the GAO/STO samples with a GAO layer thickness of 2.5 and 2.75 unit cells (uc).

a characteristic structure in the vicinity of the LO plasma frequency, ω_{LO}. The Berreman mode is conveniently presented and analyzed in terms of the difference spectrum of the ellipsometric angle, $\Psi = \arctan(r_p/r_s)$, of the heterostructure with respect to the bare STO substrate, $\Delta\Psi = \Psi(\text{sample}) - \Psi(\text{STO})$. In the following we discuss primarily the data on the sample GAO-2.5 since virtually identical results (within the accuracy of our technique) have been obtained for the sample GAO-2.75 (see figs. 2(a) and (b)). The spectrum of $\Delta\Psi$ shown in fig. 2(a) reveals two major features. The broad peak with a maximum near 956 cm^{-1} corresponds to the Berreman mode. It has been previously pointed out that the difference in frequency between this maximum and ω_{LO}(STO) is a measure of the plasma frequency of the itinerant electrons, ω_{pl} [13]. The intensity of this peak is determined by the overall sheet carrier density and its broadening by the mobility (or the inverse scattering rate). For the case of LAO/STO it was shown that this peak has a strongly asymmetric shape which provides additional information about the depth profile of the carrier concentration [13]. For the LAO/STO system the carrier density is highest next to the interface and decreases rather rapidly toward the bulk of STO over a length scale of about 11 nm. The second feature is a fairly sharp and pronounced minimum around $\omega^{dip} \approx 865\,\mathrm{cm}^{-1}$ that occurs slightly above ω_{LO}(STO) when the real part of the dielectric function of STO matches the one of the ambient such that the interface becomes fully transparent. As was outlined in ref. [19] and ref. [13], this dip feature contains contributions from the out-of-plane and the in-plane components of the dielectric function. The in-plane contribution arises from the Drude-like response of the itinerant electrons which leads to a reduction of ε_1 (865 cm^{-1}) and, given a low mobility and thus large scattering rate, an increase of ε_2 (865 cm^{-1}). The strength of this dip is a measure of the overall carrier density N_s, it is rather insensitive to the details of the depth distribution of the itinerant carriers (since the penetration depth of the infrared light is about one micrometer). It is also not sensitive to the in-plane mobility of the carriers, unless it is very low such that the Drude peak in ε_2 is very

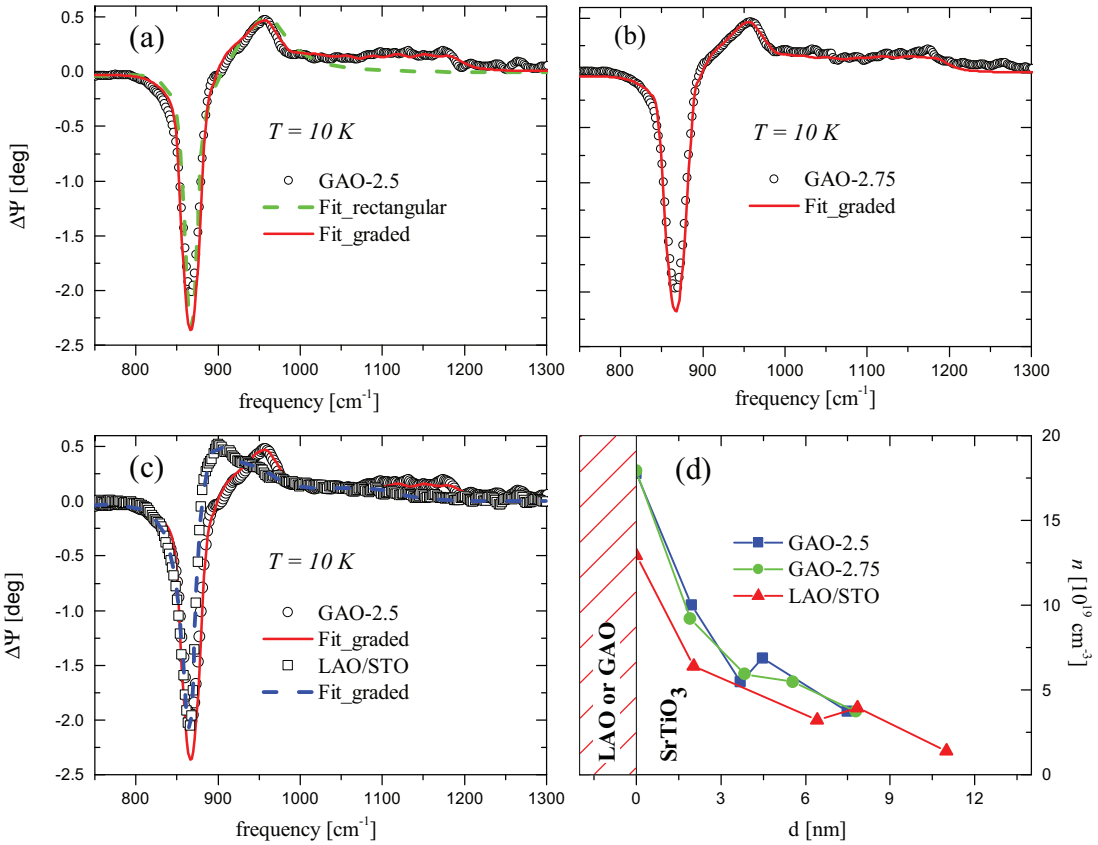

Fig. 2: (Colour online) (a) and (b) Difference spectrum of the ellipsometric angle, $\Delta\Psi = \Psi(\text{GAO/STO}) - \Psi(\text{STO})$, showing the Berreman mode above the highest LO phonon mode of STO for samples GAO-2.5 and GAO-2.75, respectively. The experimental data (open symbols) are compared with the fits with an isotropic model using a rectangular carrier concentration profile (dashed line) and a graded profile (solid line), respectively. (c) Comparison of the data and fit of GAO-2.5 with the experimental data on LAO/STO (symbols) and the best fit with a graded profile (dashed line) as reproduced from ref. [13]. (d) Comparison of the depth profile of the carrier concentration, n, as obtained from the fits with the graded potential.

Table 1: Parameters obtained from the best fit with an isotropic Drude response and a graded potential of the confined charge carriers at 10 K. The parameters for LAO/STO have been reproduced from ref. [13].

	N_s (cm^{-2})	μ (cm^2/Vs)	d (nm)
LAO/STO	5.4×10^{13}	34	11
GAO/STO - 2.5 uc	6.2×10^{13}	74	7.5
GAO/STO - 2.75 uc	6.0×10^{13}	63	7.7

broad and extends to the dip feature. We start by analyzing the ellipsometric spectra with the same model that was used in ref. [13] for the LAO/STO heterostructures. Figure 2(a) shows for GAO-2.5 the measured spectrum of $\Delta\Psi$ (symbols) at 10 K and the best fits using either a block-like potential with a constant (dashed line) or a graded profile of the concentration of the confined carriers (solid line). In the latter case, the thickness parameter, d, corresponds to the total width of the region over which the carriers are distributed. The graded profile provides a significantly better fit to the data. It reproduces the main features, like the pronounced dip around 865 cm^{-1}, the maximum around 955 cm^{-1} and, especially, the long tail toward higher frequency which is terminated by a step-like feature around 1186 cm^{-1}. Figure 2(b) shows the corresponding data and fit for GAO-2.75 which are very similar to the ones of GAO-2.5. Figure 2(c) shows a comparison with the data of GAO-2.5 and the best fit with the graded profile for the LAO/STO heterostructure [13]. The obtained depth profiles for GAO/STO (squares) and the LAO/STO (triangles) heterostructures are displayed in fig. 2(d). The derived values for the sheet carrier density N_s, the mobility, μ, and the total thickness of the conducting layers, d, are listed in table 1. To allow for a direct comparison, we assumed the same value of the effective mass, $m^* = 3.2\ m_e$, (m_e is the free electron mass) as in ref. [13]. First of all, we notice that the obtained sheet carrier density from this infrared experiment

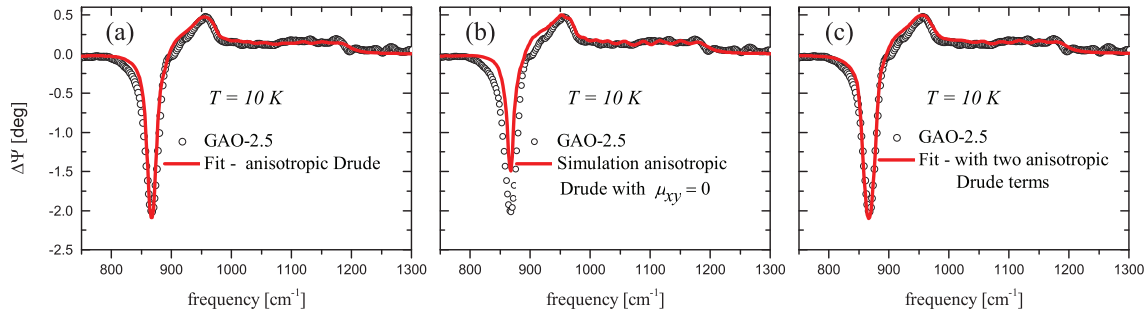

Fig. 3: (Colour online) Fitting of the difference spectrum $\Delta\Psi = \Psi(\mathrm{GAO/STO}) - \Psi(\mathrm{STO})$ with anisotropic Drude models. (a) Fit using a single anisotropic Drude term with μ_{xy} as fit parameter and the remaining parameters fixed to the values obtained from the isotropic fit as shown in fig. 2 and table 1. (b) Simulation of only the contribution of the out-of-plane component, *i.e.* for $\mu_{xy} = 0\,\mathrm{cm}^2/\mathrm{Vs}$. (c) Fit using two unidirectional Drude terms, one for the out-of-plane response with $\mu_z = 74\,\mathrm{cm}^2/\mathrm{Vs}$ and $\mu_{xy} = 0\,\mathrm{cm}^2/\mathrm{Vs}$ and the other for the in-plane response with $\mu_z = 0\,\mathrm{cm}^2/\mathrm{Vs}$ and $\mu_{xy} > 0\,\mathrm{cm}^2/\mathrm{Vs}$.

of $N_s(IR) \approx 6.2 \times 10^{13}\,\mathrm{cm}^{-2}$ and $6.0 \times 10^{13}\,\mathrm{cm}^{-2}$ for GAO-2.5 and GAO-2.75 compare indeed rather well to the ones of the dc Hall transport measurements at 10 K of $N_{s,T} \approx 1.4 \times 10^{14}\,\mathrm{cm}^{-2}$ and $5.7 \times 10^{13}\,\mathrm{cm}^{-2}$, respectively. Secondly, we remark that the larger thickness of the conducting layer of $d = 7.5\,\mathrm{nm}$, as compared to the one deduced from XPS measurements at room temperature of $d = 0.9\,\mathrm{nm}$ [10,12], can be understood in terms of the increase of the dielectric constant of STO at low temperature which leads to enhanced screening and thus a weaker confinement of the electrons. A similar difference between the thicknesses deduced from the infrared measurements at 10 K [13] and XPS [20] and scanning probe measurement at room temperature [21] was previously observed for LAO/STO. Overall, it is rather striking that despite the supposedly different origin of the confined electrons, oxygen vacancies in GAO/STO and the polar discontinuity in LAO/STO, respectively, the values of N_s and the shape of the depth profile are similar for both systems. The only main differences with respect to LAO/STO concern the thickness, d, which is somewhat reduced, and the mobility of the charge carriers, which is nearly doubled. The higher mobility enhances the visibility of the characteristic features of the Berreman mode such as the peak and, especially, the step-like edge that terminates the high-energy tail at $1185\,\mathrm{cm}^{-1}$. The latter is a measure of the maximal plasma frequency next to the interface. Note that the obtained mobility is still orders of magnitude lower than the values deduced from dc transport measurements [10]. Also, the factor of three difference in the dc mobility at 10 K of the samples GAO-2.5 and GAO-2.75 (see fig. 1) is not reflected in the value of the infrared mobility. A corresponding discrepancy between the values of the mobility obtained from dc transport and from Berreman mode in the infrared was observed for LAO/STO where it was explained in terms of the different frequency scales that are probed by the dc transport and the optical experiment. The charge carriers in bulk STO are indeed well known to have a polaronic character [22] with a strongly enhanced inelastic scattering rate in the frequency range of the Berreman mode. Our infrared data therefore suggest that the confined carriers in both GAO/STO and LAO/STO have a similar polaronic character.

While this isotropic model accounts for the main features of the Berreman mode, it fails to describe some details of the $\Delta\Psi$ curve. In particular, it overestimates the depth of the dip feature at $865\,\mathrm{cm}^{-1}$. In the following we show for the example of the GAO-2.5 samples that the fitting can be further improved by allowing for an anisotropic mobility of the charge carriers along the out-of-plane and the in-plane directions, *i.e.* $\mu_z \neq \mu_{xy}$. It is well indeed known that the confined electrons at the STO interface may originate from different bands derived from the Ti t_{2g} orbitals which have an anisotropic dispersion behavior. As was discussed in the previous paragraph, the peak of the Berreman mode is governed by the out-of-plane component of the dielectric function to which the electrons in the d_{xz}- and d_{yz}-related bands provide the major contribution since they are dispersive along the z-direction. The contribution of the d_{xy}-related bands is expected to be less important, since their z-axis conductivity arises mainly from transitions between the different subbands [18]. On the other hand, it can be expected that the electrons with d_{xy} character govern the Drude-like response along the in-plane direction which makes a major contribution to the dip feature at $865\,\mathrm{cm}^{-1}$. Figure 3(a) shows the best fit with an anisotropic Drude model, for which the mobility along the in-plane direction, μ_{xy}, was allowed to vary, whereas μ_z and N_s as well as the depth profile where kept fixed at the values obtained with the isotropic model. This anisotropic model provides a better description of the dip feature than the graded isotropic model in fig. 2(a). However, it yields an unreasonably low value of $\mu_{xy} = 5\,\mathrm{cm}^2/\mathrm{Vs}$ in view of the very high mobility that has been deduced from the dc measurements in ref. [10]. As a next step, we therefore allowed for two Drude components to account independently for the out-of-plane response (with $N_{s,z}$, $\mu_z > 0$ and $\mu_{xy} = 0$) and the in-plane response (with $N_{s,xy}$, $\mu_{xy} > 0$ and $\mu_z = 0$), respectively. The parameters $N_{s,xy}$ and μ_{xy} were allowed to vary, whereas $N_{s,z}$ and μ_z as well as the depth profile of

Table 2: Parameters obtained from the best fit to the data of GAO-2.5 using an anisotropic Drude response of the confined charge carriers along the out-of-plane (z) and the in-plane (xy) directions. Details are described in the text.

	N_s (cm^{-2}) for z-direction	N_s (cm^{-2}) for xy-direction	μ_{xy} (cm^2/Vs)
Single-component model	6.2×10^{13}	–	5
Two-component model	6.2×10^{13}	4.6×10^{13}	> 30

the carrier concentration were fixed to the ones obtained from the isotropic model. The contribution of only the z-component, which has been singled out by setting $\mu_{xy} = 0\,\mathrm{cm}^2/\mathrm{Vs}$, is shown by the red line in fig. 3(b). It confirms that the Berreman mode, *i.e.* the region above the dip where $\Delta\Psi > 0$, is indeed governed by the z-component whereas the in-plane component mainly affects the dip feature. Note that the fitting is not sensitive to the depth profile of the in-plane component. Therefore, we used for the in-plane component a block-like depth profile with a thickness of 7.5 nm. The best fit shown in fig. 3(c) yields a lower in-plane value of $N_{s,xy} = 4.6 \times 10^{13}\,\mathrm{cm}^{-2}$ and a larger mobility of $\mu_{xy} > 30\,\mathrm{cm}^2/\mathrm{Vs}$. According to the discussion in the previous paragraph, the fitting only yields a lower limit for the in plane mobility since it looses sensitivity when the Drude peak becomes too narrow. The fit in fig. 3(c) provides a satisfactory description of the experimental data that could not be significantly improved by allowing additional parameters to vary. A corresponding anisotropic fitting procedure for the LAO/STO heterostructure is not reported here since the broadening of the characteristic features of the Beremann mode, due to the lower electron mobility of LAO/STO, makes the distinction between the out-of-plane and the in-plane components more difficult and rather unreliable.

We have thus obtained the following information about the high-mobility electrons in GAO-2.5. From the analysis of the Berreman mode in the range where $\Delta\Psi > 0$, we derived the parameters of the z-axis component of the response of the carriers with $N_{s,z} = 6.2 \times 10^{13}\,\mathrm{cm}^{-2}$ and $\mu_z = 75\,\mathrm{cm}^2/\mathrm{Vs}$ and determined the shape of the graded depth profile of the carrier concentration which has a thickness of $d = 7.5\,\mathrm{nm}$. In comparison, we have obtained only limited information about the in-plane response. The latter is mostly based on the analysis of the dip feature around $865\,\mathrm{cm}^{-1}$ and yields $N_{s,xy} = 4.6 \times 10^{13}\,\mathrm{cm}^{-2}$ and a lower limit for the in-plane mobility of $\mu_{xy} > 30\,\mathrm{cm}^2/\mathrm{Vs}$ (see table 2). The width and the shape of the depth profile of the carriers that are mobile in the lateral direction along the interface could not be determined. The comparison with the LAO/STO heterostructures thus yields very similar values of N_s and the same characteristic, asymmetric shape of the depth profile. The main difference concerns the somewhat higher mobility of the confined electrons and the reduced thickness of their distribution near the interface. The reduced thickness of the conducting layer likely reflects a somewhat larger magnitude of the confining potential (that is consistent with the slightly larger value of N_s) rather than a reduced strength of the dielectric screening in STO. The latter would require a hardening of the soft mode in STO that results from defects and compressive strain which both are expected to be stronger in LAO/STO than in GAO/STO. The twofold increase of the mobility in GAO/STO, as compared to the one in LAO/STO, is still much smaller than the corresponding increase of the dc mobility as obtained from the transport measurements which amounts to more than an order of magnitude. Furthermore, despite a threefold difference in the dc mobility of the samples GAO-2.5 and GAO-2.75, the mobility values obtained from the analysis of the Berreman mode are comparable. These trends can be understood in terms of the polaronic nature of the electrons in STO which leads to a strong inelastic interaction with the lattice in the frequency range of the Berreman mode. Apparently, this polaronic coupling is less sensitive to defects and strain than the elastic scattering processes that governs the dc mobility.

Summary. – With infrared ellipsometry we have studied the so-called Beremann mode in GAO/STO heterostructures which arises from the itinerant charge carriers that are confined to the interface. We analyzed the Beremann mode with the same model that was previously used in ref. [13] for LAO/STO heterostructures and found that both kinds of samples have a similar sheet carrier densities and asymmetric shapes of the depth profile of the carrier concentration, although the main origin of the confined carriers is supposed to be different, *i.e.* oxygen vacancies in GAO/STO and a polar discontinuity in LAO/STO. The most significant differences concern the mobility of the charge carriers, which is twice higher in GAO/STO, and the thickness of the depth profile of the confined electrons which is somewhat redcued. The stronger carrier confinement in the GAO/STO heterostructure may be the result of a larger confining potential [12]). The observed twofold increase of the mobility deduced from the Berreman mode is still much smaller than the one of the dc mobility which is more than tenfold. This can be understood in terms of a polaronic nature of the confined electrons in STO (similar to the one in bulk STO [22]).

* * *

The work at the University of Fribourg has been supported by the Schweizerische Nationalfonds (SNF)

through the grant No. 200020-153660. The work at Muni was supported by the project CEITEC (CZ.1.05/1.1.00/02.0068). Funding from the Danish Agency for Science, Technology and Innovation (4070-00047B) is also acknowledged.

REFERENCES

[1] Mannhart J. *et al.*, *MRS Bull.*, **33** (2008) 1027.
[2] Cen C. *et al.*, *Science*, **323** (2009) 1026.
[3] Caviglia A. D. *et al.*, *Nature*, **456** (2008) 624.
[4] Willmott P. R. *et al.*, *Phys. Rev. Lett.*, **99** (2007) 155502.
[5] Kalabukhov A. *et al.*, *Phys. Rev. B*, **75** (2007) 121404.
[6] Herranz G. *et al.*, *Sci. Rep.*, **2** (2012) 758.
[7] Chen Y. Z. *et al.*, *Nano Lett.*, **11** (2011) 3774.
[8] Lee S. W. *et al.*, *Nano Lett.*, **12** (2012) 4775.
[9] Liu Z. Q. *et al.*, *Phys. Rev. X*, **3** (2013) 021010.
[10] Chen Y. Z. *et al.*, *Nat. Commun.*, **4** (2013) 1371.
[11] Kormondy K. J. *et al.*, *J. Appl. Phys.*, **117** (2015) 095303.
[12] Schütz P. *et al.*, *Phys. Rev. B*, **91** (2015) 165118.
[13] Dubroka A. *et al.*, *Phys. Rev. Lett.*, **104** (2010) 156807.
[14] Bernhard C. *et al.*, *Thin Solid Films*, **455** (2004) 143.
[15] Kozuka Y. *et al.*, *Phys. Rev. B*, **76** (2007) 085129.
[16] Berreman D. W. *et al.*, *Phys. Rev.*, **130** (1963) 2193.
[17] Humlíček J. *et al.*, *Appl. Phys. Lett.*, **69** (1996) 2581.
[18] Rössle M. *et al.*, *Phys. Rev. B*, **88** (2013) 104110.
[19] Park S. Y. *et al.*, *Phys. Rev. B*, **87** (2013) 205145.
[20] Sing M. *et al.*, *Phys. Rev. Lett.*, **102** (2009) 176805.
[21] Basletic M. *et al.*, *Nat. Mater.*, **7** (2008) 621.
[22] van Mechelen J. L. M. *et al.*, *Phys. Rev. Lett.*, **100** (2008) 226403.